

LANGLEY  
SCD  
11-75-3R  
1988  
198

**Final Technical Report**  
**NASA/Langley Contract No. NAG-1-851**  
**August 2, 1988 - February 2, 1989**

A. K. Wahi, I. Lindau, and W. E. Spicer  
*Stanford Electronics Laboratory, Stanford University, Stanford, CA 94305*

## I. Introduction

Studies of metal interface formation on HgCdTe have pointed to the influence of the weak Hg-Te bond and the consequent ease of Hg loss as a major factor contributing to semiconductor disruption and metal-semiconductor intermixing that occurs upon metal deposition<sup>1</sup>. The disruption and interfacial instabilities that result prove deleterious to device stability and performance. We have initiated a study examining interface morphology and band bending behavior in the binary compounds CdTe and ZnTe. By focusing on the binaries, where the effects of Hg loss are absent, we gain further insight into the role of Hg loss during interface formation. Cation Cd (or Zn) behavior can also be examined, and any differences in interfacial chemistry and morphology associated with the Zn may be studied and give possible clues as to what might be expected for the same metals on HgZnTe. Determining Fermi level pinning behavior in these two binaries also has important implications for the corresponding metal/Hg<sub>1-x</sub>Cd<sub>x</sub>Te and metal Hg<sub>1-x</sub>Zn<sub>x</sub>Te interfaces. As discussed by Spicer *et al.*<sup>2</sup>, the Fermi level pinning positions at the two binary extremes of alloy composition may be extrapolated through the range of alloy compositions. Thus this knowledge can be used to predict the electrical behavior of metal contacts to the alloys HgCdTe and HgZnTe.

In Section II, we present results from our comparative study of the Al, Ag, and Pt interfaces with CdTe and ZnTe<sup>3</sup>. Results are compared to metal/HgCdTe interface formation, and we consider implications for metal/HgZnTe interfaces.

## References

1. D. J. Friedman, G. P. Carey, I. Lindau, W. E. Spicer, and J. A. Wilson, *J. Vac. Sci. Technol. B* 4, 980 (1986).
2. W. E. Spicer, D. J. Friedman, and G. P. Carey, *J. Vac. Sci. Technol. A* 6, 2746 (1988).
3. A. K. Wahi, G. P. Carey, T. T. Chiang, I. Lindau, and W. E. Spicer, *J. Vac. Sci. Technol.*, to be published.

(NASA-CR-184840) RESEARCH AND DEVELOPMENT  
OF HgZnTe AS AN INTERFACED MATERIAL Final  
Technical Report, 2 Aug. 1988 - 2 Feb. 1989  
(Stanford Univ.) 19 F CSCI 20L

N89-20820

Unclas  
H1/76 0198639

## CdTe and ZnTe Metal Interface Formation and Fermi Level Pinning

A. K. Wahi, G. P. Carey, T. T. Chiang, I. Lindau, and W. E. Spicer<sup>a)</sup>  
*Stanford Electronics Laboratory, Stanford University, Stanford, CA 94305*

### Abstract

Interfacial morphology and Fermi level pinning behavior at the interfaces of Al, Ag, and Pt with UHV-cleaved CdTe and ZnTe have been studied using x-ray and ultraviolet photoemission spectroscopies. Results are compared to metal/HgCdTe interface formation, where the weak Hg-Te bond and consequent ease of Hg loss strongly influence semiconductor disruption and metal-semiconductor intermixing. For Al/CdTe, the strong Al-Te reaction yields a significantly more extensive Al-Te reacted region than has been observed for HgCdTe. The Al/ZnTe interface is observed to be more abrupt than Al/CdTe. The final Fermi level pinning positions  $E_{fi} = E_f - E_{vbm}$  for Al, Ag, and Pt on *p*-type CdTe and *p*-ZnTe have been determined.  $E_{fi}$  is found to be roughly the same for both CdTe and ZnTe, with the value for ZnTe lying approximately 0.2 eV closer to the VBM for all three metals. From these results, one would expect Schottky barriers of about the same height for these metals on *p*-CdTe and *p*-ZnTe; and also that, in principle, metal interfaces with the two alloys HgCdTe and HgZnTe would have the same properties. Comparisons and implications for electrical behavior of metal contacts to the alloys are discussed.

## I. Introduction

Studies of metal/HgCdTe interface formation have pointed to the weak Hg bonding in HgCdTe as an important factor contributing to the significant semiconductor disruption and metal-semiconductor intermixing that occurs when metals are deposited onto surfaces of UHV-cleaved HgCdTe<sup>1</sup>. Hg depletion ranging from 20 to 60% from the near-surface region after deposition of only a few monolayers (ML) of metal is typically observed. The resulting disruption and interfacial instabilities at metal contacts to HgCdTe prove deleterious to device stability and performance. The related alloy HgZnTe has been proposed as a substitute IR detector material<sup>2</sup> with potentially greater lattice stability than HgCdTe, and it is therefore of interest to compare the behavior of metal contacts to both alloys.

We have studied metal interfaces formed on CdTe and ZnTe in order to investigate interfacial morphology in conjunction with Fermi level pinning behavior at metal coverages from submonolayer to tens of monolayers. Studying the behavior of these related binary semiconductors where the effects of Hg loss are absent gives insight into the role of the weak Hg-bonding in the alloy. Fermi level pinning positions in the binaries are also used<sup>3</sup> to predict and make comparisons between electrical properties of metal contacts to the alloys HgCdTe and HgZnTe.

The metals Al, Ag, and Pt were chosen to provide a range of reactivities with the substrate. The relevant bulk thermodynamic parameters for interfaces with these metals provide a useful guide for predicting the interfacial chemistry that might be observed, and, in general for metal/HgCdTe systems, the chemistry observed has been consistent with these predictions. Al is highly reactive with Te [ $\Delta H_f(\text{Al}_2\text{Te}_3) = -76.1$  kcal/mol] and Ag and Pt comparatively non-reactive with Te [ $\Delta H_f(\text{Ag}_2\text{Te})$  and  $\Delta H_f(\text{PtTe}) = -8.6$  and  $-10.0$  kcal/mol, respectively]<sup>4</sup>. For both Al and Ag, calculations using the semi-empirical model of Miedema<sup>5</sup> predict a minimal driving force for cation (Cd or Zn) alloying with the overlayer metal, whereas strong cation alloying behavior with Pt is expected<sup>6</sup>. Because of the similar heats of formation for CdTe and ZnTe [ $\Delta H_f(\text{CdTe}) = -24.1$  kcal/mol and  $\Delta H_f(\text{ZnTe}) = -28.5$  kcal/mol], the interfacial chemistry and morphology for

each of these metals on both semiconductors is expected to be similar. In comparison to CdTe, the weak Hg bonding in HgCdTe [reflected in the small  $\Delta H_f(\text{HgTe}) = -7.6$  kcal/mol] and consequent ease of Hg loss is expected to result in more disruptive interfaces. Here we emphasize interface morphology for Al/CdTe and Al/ZnTe. For Al, significantly greater intermixing occurs in CdTe than seen on HgCdTe. The Al/ZnTe interface is also more abrupt than Al/CdTe. We also present band bending results for interfaces of all three metals with *p*- CdTe and *p*- ZnTe and consider implications for metal/HgZnTe interface formation.

## II. Experimental Procedure

Single crystal bars of CdTe (both *p*- and *n*- type) and *p*- ZnTe (ZnTe obtained from Cleveland Crystals, Inc.), with cross-sectional areas of  $5 \times 5 \text{ mm}^2$  for CdTe and  $2.5 \times 2.5 \text{ mm}^2$  for ZnTe, were introduced into a previously baked UHV chamber and then cleaved in vacuum (with base pressure  $< 1 \times 10^{-10}$  torr) to reveal atomically clean (110) surfaces. Sequential metal depositions were performed by evaporation from a tungsten filament, with metal coverage monitored using a quartz oscillator. Experiments were performed at the Stanford Synchrotron Radiation Laboratory using synchrotron radiation with photon energies chosen for maximum surface-sensitivity, and also using conventional x-ray (Mg  $K\alpha$  and Zr  $M\zeta$ ,  $h\nu = 1253.6$  and  $151.4$  eV, respectively) and ultraviolet (He I and II,  $21.2$  and  $40.8$  eV) photon sources to provide both surface-sensitive ( $\sim 5 - 10 \text{ \AA}$  photoelectron escape depth) and bulk-sensitive ( $\sim 20 - 25 \text{ \AA}$ ) core level emission. The kinetic energy of photoemitted electrons was measured using a double-pass CMA. In addition, LEED was performed on some of these interfaces in order to monitor surface crystallinity during overlayer growth, with beam current  $\leq 1 \text{ }\mu\text{A}$ . Throughout the following, metal coverages are given in terms of a monolayer (ML), equivalent to the surface density of atoms on the (110) faces of CdTe or ZnTe ( $6.74 \times 10^{14}$  and  $7.60 \times 10^{14}$  atoms/cm<sup>2</sup>, respectively). For example, 1 ML corresponds to  $1.12 \text{ \AA}$  of Al on CdTe and  $1.26 \text{ \AA}$  of Al on ZnTe.

### III. Results

#### A. Interfacial Chemistry and Morphology: Al/CdTe and Al/ZnTe

As expected, a strong Al-Te reaction is seen for Al on CdTe and ZnTe, as has been seen in previous studies of the Al/HgCdTe interface<sup>7-8</sup>. A reacted Al-Te layer is formed, and at higher coverages metallic Al forms on top of this reacted region. While the same general chemical behavior is seen for all three systems, significant differences in morphology are seen, with the extent of this reaction on CdTe significantly greater than on either ZnTe or HgCdTe. Figure 1 shows the evolution of the Al 2*p* core level with Al coverage for Al on *n*-CdTe and *p*-ZnTe. On both CdTe and ZnTe, Al emission first emerges with higher binding energy than bulk Al metal, and this reacted Al component moves to still higher binding energy with successive Al depositions. A corresponding shifted component of Te emission, which would be indicative of a reacted Te species distinguishable from Te in bulk CdTe or ZnTe, is not seen; however, a broadening of the Te signal is observed, similar to what is seen for Al/HgCdTe. Furthermore, as described below, while Cd is not incorporated into the overlayer as it forms, Te attenuation from the surface region is very slow. We therefore ascribe this reacted Al 2*p* signal to Al reacted with Te, with Te retaining the same binding energy as in bulk CdTe (and ZnTe). At higher coverages metallic Al forms on top of this reacted layer, with a signal from unreacted Al emerging at approximately 2.5 eV lower binding energy, corresponding to the binding energy of metallic Al<sup>9</sup>. The emergence of metallic core level emission is accompanied by the appearance of Fermi level emission. On ZnTe, unreacted Al is first seen near 7 ML coverage, compared with its first appearance on HgCdTe after deposition of about 3 ML Al. On CdTe, however, only Al reacted with Te is seen up to near 40 ML on the *n*-type sample. (On the *p*-type CdTe, only reacted Al was seen up to the maximum coverage studied of 29 ML.) The dominance of the reacted Al component up to the highest coverages in CdTe suggests a strong Al reaction with a high degree of Al - Te intermixing, especially in comparison to what is seen for HgCdTe. The separation in binding energy of the reacted and metallic Al components is similar to what has been observed for Al on CdS<sup>10</sup>.

Significantly, the observed separation is greater than observed for HgCdTe, where the binding energy of the reacted Al component is only 1 to 1.5 eV higher than the metallic component<sup>7-8</sup>. Thus the reacted Al on HgCdTe emerges with intermediate binding energy which suggests that a less highly reacted species of reacted Al is formed on the alloy.

As Figure 1 shows for CdTe and ZnTe, a strong reacted Al component is present in the surface-sensitive emission (i.e., from within the top 10 Å) at even the highest metal coverages. This observation suggests that a floating layer of reacted Al - Te remains on the surface. Such a surface-segregated layer has been suggested for Al/HgCdTe<sup>7-8</sup>. Further evidence that this layer exists on CdTe is shown in Table I, which compares surface-sensitive (using Zr  $M\zeta$ ,  $h\nu = 151.4$  eV) and bulk-sensitive (using Mg  $K\alpha$ ,  $h\nu = 1253.6$  eV) Al 2p emission for the higher coverages. The bulk sensitive emission emerges with kinetic energy near 1176 eV, which corresponds to an electron escape depth of about 25 Å; while most of the surface-sensitive emission (shown in Figure 1) emerges from within the top 10 Å. The clear distinction between the metallic and reacted Al 2p peaks makes it possible to separate the reacted and unreacted contributions to the Al 2p signal, with an accuracy estimated to be within 30%. Table I gives the percent of the total Al 2p signal which is metallic for both the surface-sensitive and bulk-sensitive emission for Al on *n*-CdTe. It can be seen that the ratio of metallic Al intensity to the reacted Al intensity is greater in the more bulk-sensitive emission. Thus, there is a gradient in metallic Al concentration, with the outer surface rich in reacted Al and the amount of metallic Al increasing as one moves from the outer surface towards the substrate. The floating reacted layer here has been easy to observe more directly than in the case of Al on HgCdTe due to the thickness of the reacted layer formed on CdTe and the greater separation in binding energy between the reacted and unreacted Al 2p components.

Figure 2 shows the attenuation of core levels as a function of Al coverage for Al on *n*-CdTe. The Te 4d and Cd 4d emission is surface-sensitive, emerging from within the top 5-10 Å of the surface, whereas the Te 3d and Cd 3d emission is more bulk-sensitive. For both the bulk- and surface-sensitive Cd and Te core level emission, the signals attenuate with coverage at a rate that is slower than expected for formation of a uniform abrupt interface. In addition, in the surface

region (within the top 10 Å), the Te 4*d* signal attenuates much more slowly than the Cd 4*d* signal. The bulk Cd/Te ratio, however, does not change appreciably as more metal is deposited. That the Cd/Te ratio at the surface decreases, while the overall Cd/Te ratio remains unchanged to within a depth of ~25 Å, suggests that Te is pulled from the bulk to the near surface region, reacting with Al. The slow overall attenuation of the substrate signal can be accounted for by islanding of the overlayer as it grows or intermixing of components. There is evidence of initial islanding of Al on the surface found in the LEED pattern, which persists beyond 5 ML Al coverage, disappearing at 10 ML.

A surprising result of this work is the lack of a Cd signal from dissociated Cd that is clearly distinguishable from the Cd signal of bulk CdTe. For example, Patterson and Williams<sup>12</sup> have reported the appearance of metallic Cd for thick overlayers of Al on CdTe, although they do not give quantitative values of thickness. For the thickness range studied here (up to 81 ML of Al), it did not appear. Although no clear evidence has been seen for elemental Cd forming at the Al/HgCdTe interface, the binding energy of any formed would not necessarily be separated from Cd in bulk HgCdTe<sup>13</sup>. However, on CdTe, a signal from any elemental Cd should be clearly resolvable, with Cd 4*d* emission from elemental Cd emerging with a binding energy of 10.6 eV relative to the Fermi level<sup>9</sup>. Emission from any Cd alloyed with the overlayer would be expected to emerge with about 0.15 eV higher binding energy than elemental Cd<sup>6</sup>; and, though this might not be easily distinguished from metallic Cd, it also should be clearly resolvable from Cd in bulk CdTe. However, as Figure 3 shows for the Cd 4*d* core level, a signal from metallic Cd or Cd alloyed with Al is not observed, and neither is it seen in the more bulk-sensitive Cd 3*d* emission. (The observed shift of the Cd 4*d* emission with Al deposition in Figure 3 is due to band bending.) Bulk thermodynamics does not favor alloying of Cd with the Al overlayer. A clear signal from Cd alloyed with the overlayer has been seen in systems where the cation exhibits strong alloying with the overlayer, e.g., for Pt and Cu overlayers on HgCdTe<sup>14</sup> and CdTe<sup>11</sup>, respectively.

Although the details of the Al reaction, with the formation of a surface-segregated reacted layer on top of an eventually metallic overlayer, are essentially the same in both CdTe and ZnTe, the extent of this reaction on CdTe is significantly greater.

### B. Band Bending

In Table II we give our measured values for the final surface Fermi level pinning positions relative to the valence band maximum,  $E_{fi} = E_f - E_{vbm}$ , for the metals Al, Ag, and Pt on vacuum-cleaved surfaces of *p*-type CdTe and *p*-type ZnTe. The movement of the Fermi level relative to the VBM is determined by shifts in the core levels, which can be measured very precisely, as a function of metal coverage. The VBM position for CdTe is then located  $10.25 \pm 0.05$  eV above the position of the Cd  $4d\ 5/2$  core level, and the ZnTe VBM is located  $9.75 \pm 0.05$  eV above the position of the Zn  $3d$  core level, as determined using angle-resolved photoemission<sup>15</sup>. We find that for CdTe and ZnTe (with very different bandgaps of, for CdTe and ZnTe,  $E_g = 1.5$  eV and 2.2 eV, respectively), for each of these metals, the Fermi level pins at roughly the same distance from the VBM in both CdTe and ZnTe. We note in addition that the ZnTe value lies at about 0.2 eV closer to the VBM than CdTe for all three metals. The as-cleaved position of  $E_f$  for ZnTe was  $\sim 0.4$  eV above the VBM for all three cleaves; for CdTe,  $E_{fi}$  on the cleaved surfaces was about 0.5 eV for the Al and Pt cleaves and 0.65 for the Ag cleave. Upon metal deposition,  $E_f$  moves from its position at the cleave up towards the CBM. In the case of Ag/ZnTe, the Fermi level moves up with coverage to 0.8 eV above the VBM and then down to the final position listed in Table II. For Al and Pt, the Fermi level position stabilized below 1 ML coverage for both CdTe and ZnTe. Below we discuss the various models for Fermi level pinning behavior at metal/semiconductor interfaces that might agree with the observed difference in pinning positions. As we will discuss, an interesting point is that the movement of the Fermi level in the reactive Al/CdTe system is complete before the appearance of any metallic Al in the spectra, and therefore effects dependent upon the metallicity of the overlayer appear to be ruled out in this case.



## IV. Discussion

### A. Al on CdTe, ZnTe, and HgCdTe

The differences seen in the extent of the reaction on CdTe and HgCdTe, and the more highly reacted Al component seen in CdTe compared to HgCdTe, are not explained from a consideration of bulk thermodynamic parameters alone. Since in HgCdTe, a reactive metal such as Al can remove Te from Hg more easily than from Cd or Zn, and rapid Hg loss provides a ready source of Te, a more extensive Al-Te reaction might be expected to occur. Clearly this is not the case. Instead, the kinetics at the HgCdTe interface may be dominated by the disruption due to Hg depletion, determining the extent of reaction and intermixing of semiconductor components with the overlayer metal. For instance, after only a few ML of Al are deposited onto HgCdTe<sup>7-8</sup>, at least 50% of the Hg is already lost from the first approximately 30 Å of the substrate surface. Such rapid Hg loss would be expected to result in significant disorder, with possibly a collapse of the lattice. The rapid depletion of Hg from the lattice then slows, to a rate expected for attenuation of the Hg signal through an overlayer<sup>8</sup>. Formation of a barrier to further movement of semiconductor components due to inhibited diffusion of Hg through the disrupted region can explain the less extensive reacted region seen for Al/HgCdTe in comparison to CdTe.

While the presence of Hg can account for the difference in behavior observed between Al/HgCdTe and Al/CdTe, the difference in behavior between ZnTe and CdTe is surprising, when simple considerations of bulk thermodynamics predict the same behavior for both.

### B. Band Bending

From the rough similarity in  $E_{fi}$  for CdTe and ZnTe listed in Table II, one would expect for these metals Schottky barriers of roughly the same height on both *p*-CdTe and *p*-ZnTe. We note, however, that the ZnTe value lies at about 0.2 eV closer to the VBM than CdTe for all three metals. In speculating on possible models which would be consistent with this result, we focus on the two models most often used to interpret Fermi level movement with metal coverage: the metal-induced gap states (MIGS) model, in which tailing of the metal wavefunctions into the semiconductor

produce states in the bandgap that pin the Fermi level; and defect models, in which the defect energy levels responsible for the observed pinning in CdTe and ZnTe would lie at nearly the same energy with respect to the VBM in both semiconductors. The observed difference in pinning positions for CdTe and ZnTe is consistent with MIGS models, which predict that a difference in  $E_{\text{fi}}$  for two semiconductors will be observed which depends on their band lineup<sup>16</sup>, i.e., that the difference in Schottky barrier height for two semiconductors will be given by their valence band offset. The measured ZnTe - CdTe valence band offset has been determined<sup>15</sup> as  $0.18 \pm .06$  eV, with the ZnTe VBM lying above that of CdTe, in agreement with what is seen here. However, for the case of Al on CdTe and ZnTe, band bending is completed below 1 ML, well before established Fermi level emission and a metallic Al component is seen. Consequently a MIGS-type mechanism, which depends upon the metallicity of the overlayer, appears to be ruled out in this instance, and a defect mechanism is favored. Calculations for bulk defects in the HgTe - CdTe system are available from the work of Kobayashi *et al.*<sup>17</sup>. We focus on defects involving Te in view of the frequently observed outdiffusion of Te from the lattices of both HgCdTe<sup>7,14,18</sup> and CdTe<sup>11</sup> upon metal deposition. From their work, a likely candidate involved in Fermi level movement in CdTe might be the  $\text{Te}_{\text{Cd}}$  antisite, with an energy about 1 eV above the VBM. This defect could account for the observed narrow range of Fermi level pinning positions ranging from 0.7 - 1.1 eV above the VBM seen for CdTe<sup>11</sup>. Alternatively, a possibility for an intrinsic defect which might be involved is the Te vacancy, which is predicted to be a shallow double donor in CdTe<sup>19</sup>. Comparison with ZnTe is hampered by the lack of available calculations specifically for this system, however one might speculate that similar defects occur here as well. Although extensive work is reported in the literature for Schottky barrier heights and Fermi level pinning positions for a wide range of metals on CdTe, there is a lack of available theoretical work on surface defects in II-VI materials. Clearly a much greater understanding is desirable.

One can extrapolate from the Fermi level pinning position in the binaries through the range of alloy compositions  $\text{Hg}_{1-x}\text{Cd}_x\text{Te}$  and  $\text{Hg}_{1-x}\text{Zn}_x\text{Te}$  to obtain predictions for the electrical behavior of metal/HgCdTe and metal/HgZnTe interfaces. Several different models for Fermi level pinning

may be used, as discussed by Spicer *et al.*<sup>3</sup>, and these yield similar predictions, that ohmic contacts will be obtained for metals on *n*- type HgCdTe below a certain *x*-value of about 0.4, and that rectifying contacts will be obtained on *p*- type HgCdTe of all compositions. The observed similarity of  $E_{fi}$  for CdTe and ZnTe lead to a prediction that metal contacts to the alloy HgZnTe would yield in principle the same properties as on HgCdTe; that is, intrinsically ohmic contacts will be obtained on *n*- type HgZnTe below a certain *x*-value, with perhaps a lower crossover value of  $x = 0.3$  due to the larger bandgap of HgZnTe, and rectifying contacts will be obtained on *p*- type HgZnTe of all compositions. For Fermi level pinning in the Hg-containing alloys, however, additional mechanisms for Fermi level movement are possible that are not present in CdTe and ZnTe which involve Hg loss. These mechanisms involve metal movement into the semiconductor via Hg vacancies, and the resultant doping of the substrate<sup>6,20</sup>.

## V. Conclusions

In summary, the Al, Ag, and Pt interfaces with CdTe and ZnTe have been investigated in a comparative study of CdTe and ZnTe metal interface morphology and Fermi level pinning behavior. For reactive Al overlayers, a more disruptive interface with a higher degree of intermixing occurs in the binary CdTe than has been seen for the Al/HgCdTe interface. The extent of the Al reaction with Te is inhibited in the Hg-containing alloy due to the disruption due to Hg loss. The Fermi level pinning positions,  $E_f - E_{vbm}$ , for Al, Ag, and Pt on *p*- type CdTe and *p*- ZnTe are found to be roughly the same, with the values for ZnTe lying about 0.2 eV closer to the VBM for each metal. From these results, similar electrical behavior for metal contacts to the alloys HgCdTe and HgZnTe is expected.

**Acknowledgment:** Work supported by NASA/Langley under contract # NAG1-851 and by DARPA under contract # N00014-86-K0854. This work was partially performed at the Stanford Synchrotron Radiation Laboratory which is funded by the DOE under contract DE-AC03-82ER-13000, Office of Basic Energy Sciences, Division of Chemical/Material Sciences.

### References

- a) Stanford Ascherman Professor of Engineering.
1. D. J. Friedman, G. P. Carey, I. Lindau, W. E. Spicer, and J. A. Wilson, *J. Vac. Sci. Technol. B* **4**, 980 (1986).
  2. A. Sher, A.-B. Chen, W. E. Spicer, and C.-K. Shih, *J. Vac. Sci. Technol. A* **3**, 105 (1985).
  3. W. E. Spicer, D. J. Friedman, and G. P. Carey, *J. Vac. Sci. Technol. A* **6**, 2746 (1988).
  4. K. C. Mills, *Thermodynamic Data for Inorganic Sulfides, Selenides, and Tellurides* (Butterworths, London 1974).
  5. A. R. Miedema, P. F. Chatel, and F. R. de Boer, *Physica B* **100**, 1 (1980).
  6. D. J. Friedman, G. P. Carey, I. Lindau, and W. E. Spicer, *J. Vac. Sci. Technol. A* **5**, 3190 (1987). Calculations of the heat of solution of cation Cd or Hg at infinite dilution in metal M for several metals obtained using the Miedema model (ref. 5 with tabulations therein) are given here. To these we add values  $\Delta H_{\text{sol}}(\text{Zn}; \text{M})$  for Zn: Al, +0.5 kcal/mol; Ag, -4.3 kcal/mol; Pt, -30.0 kcal/mol.
  7. G. D. Davis, N. E. Byer, R. A. Riedel, and G. Margaritondo, *J. Appl. Phys.* **57**, 1915 (1985).
  8. D. J. Friedman, G. P. Carey, C. K. Shih, I. Lindau, W. E. Spicer, and J. A. Wilson, *J. Vac. Sci. Technol. A* **4**, 1977 (1986).
  9. L. Ley and M. Cardona, Eds., *Photoemission in Solids II* (Springer-Verlag, Berlin 1979).
  10. L. J. Brillson, R. S. Bauer, R. Z. Bachrach, and J. C. McMenamin, *J. Vac. Sci. Technol.* **17**(1), 476 (1980).
  11. D. J. Friedman, I. Lindau, W. E. Spicer, *Phys. Rev. B* **37**, 731 (1988).
  12. M. H. Patterson and R. H. Williams, *J. Cryst. Growth* **59**, 281 (1982).
  13. D. J. Friedman, Ph. D. Thesis, Stanford University, 1987.
  14. D. J. Friedman, G. P. Carey, I. Lindau, W. E. Spicer, *Phys. Rev. B* **35**, 1188 (1987).

- 
15. C. K. Shih, A. K. Wahi, I. Lindau, and W. E. Spicer, *J. Vac. Sci. Technol. A* **6**, 2640 (1988).
  16. J. Tersoff, *Phys. Rev. Lett.* **56**, 2755 (1986).
  17. A. Kobayashi, O. F. sankey, and J. D. Dow, *Phys. Rev. B* **25**, 6367 (1982).
  18. A. Franciosi, P. Philip, and D. J. Peterman, *Phys. Rev. B* **32**, 8100 (1985).
  19. M. S. Daw, D. L. Smith, C. A. Swarts, and T. C. McGill, *J. Vac. Sci. Technol.* **19** (3), 508 (1981).
  20. G. P. Carey, A. K. Wahi, D. J. Friedman, C. E. McCants, and W. E. Spicer, *Proceedings of the 1988 MCT Workshop, J. Vac. Sci. Technol.*, to be published.

Table I. The percent of the total Al 2p signal which is metallic for Al on *n*- CdTe. The bulk-sensitive data was taken with XPS using Mg  $K\alpha$ .

Al coverage (ML)	bulk (25 Å)	surface (10 Å)
23	0 %	0 %
46	60 %	45 %
81	79 %	67 %

Table II. Final surface Fermi level pinning positions relative to the valence band maximum,  $E_{fi} = E_f - E_{VBM}$ , for the metals Al, Ag, and Pt on vacuum cleaved surfaces of *p*- CdTe and *p*- ZnTe.

	<u><i>p</i>- CdTe</u>	<u><i>p</i>- ZnTe</u>
Al	$1.1 \pm .1$	$0.9 \pm .1$ eV
Ag	$0.85 \pm .1$	$0.65 \pm .1$ eV
Pt	$0.95 \pm .1$	$0.7 \pm .1$ eV

---

### Figure Captions

Figure 1. Surface sensitive photoemission spectra showing the evolution of the Al 2*p* core level as a function of Al coverage on (a) ZnTe and (b) CdTe. Most of the signal emerges from within the top 10 Å of the surface. At higher coverages, emission from metallic Al at lower binding energy to reacted Al is seen.

Figure 2. Attenuation of core level intensity as a function of Al coverage for Al on *n*- CdTe. The Te 4*d* emission from the surface attenuates very slowly with coverage, with Te reacting with the overlayer metal. The more rapid decrease in Cd 4*d* intensity indicates Cd is not incorporated into the Al overlayer.

Figure 3. Cd 4*d* spectra for Al on *n*- CdTe with increasing Al coverage. The observed shift is due to band bending. No evidence is seen for elemental Cd, with a binding energy of 10.6 eV relative to the Fermi level. Emission from any Cd alloyed with the overlayer would be expected to emerge with 0.15 eV higher binding energy than elemental Cd [ref. 6] and is not observed.



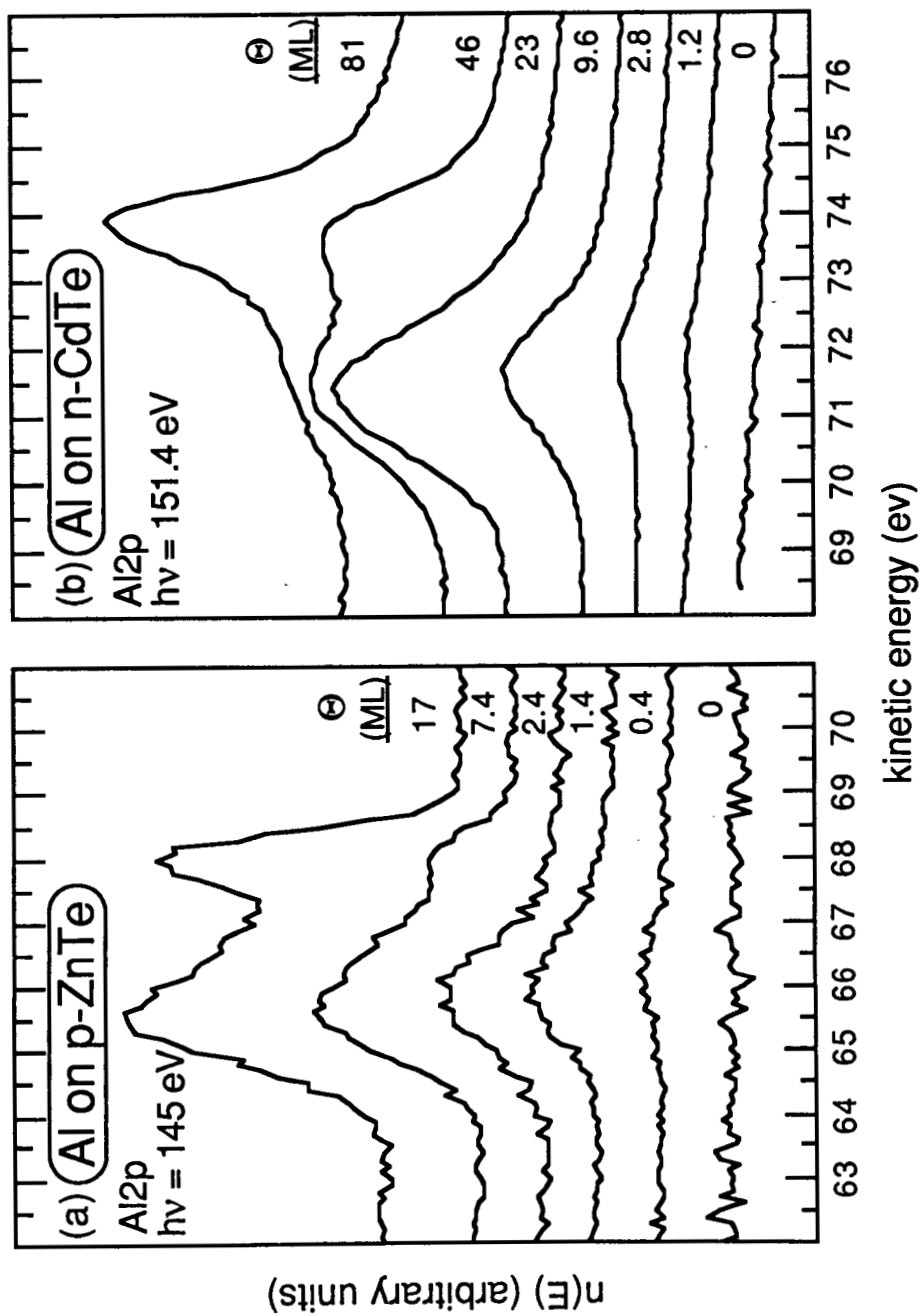


Figure 1

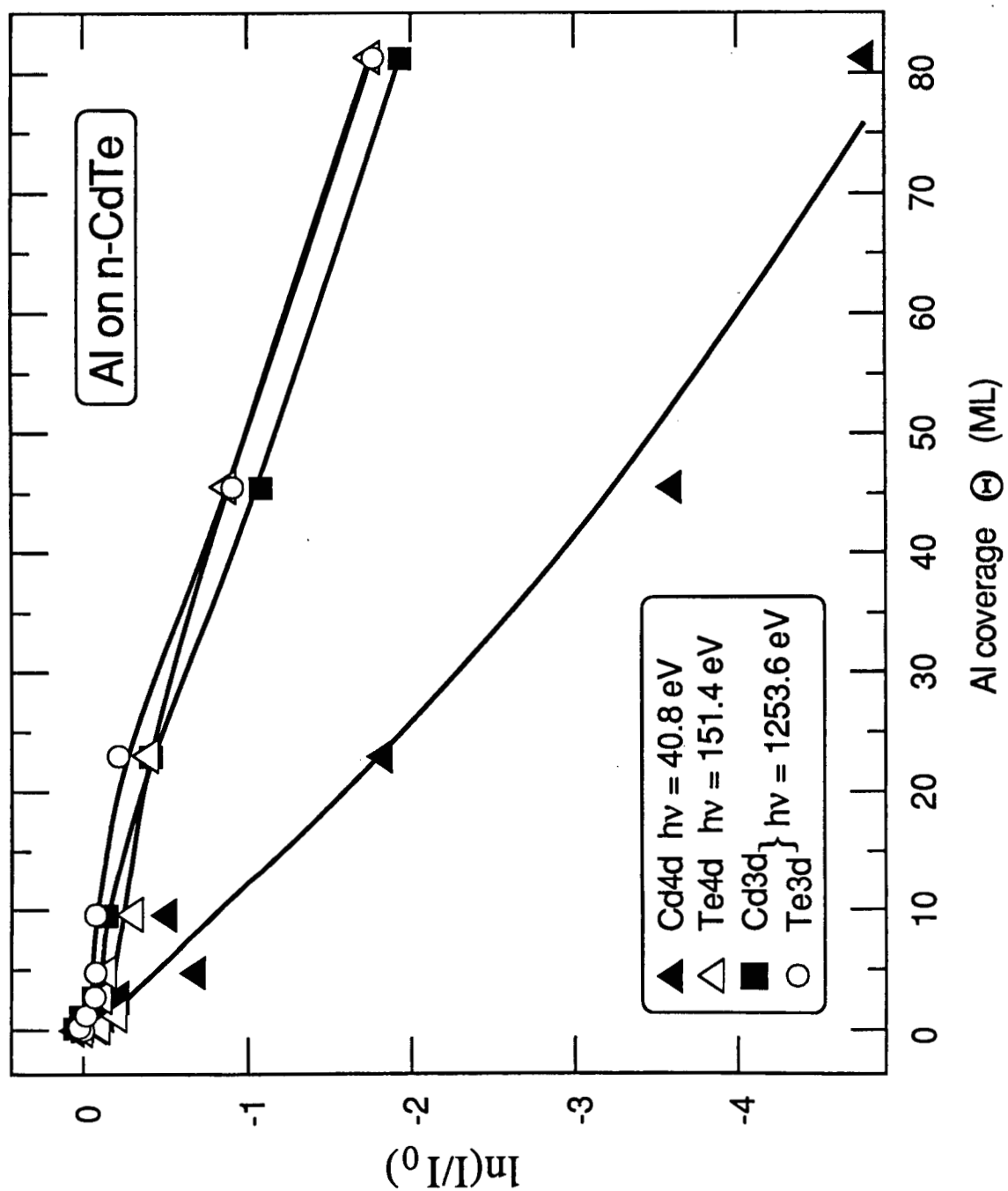


Figure 2

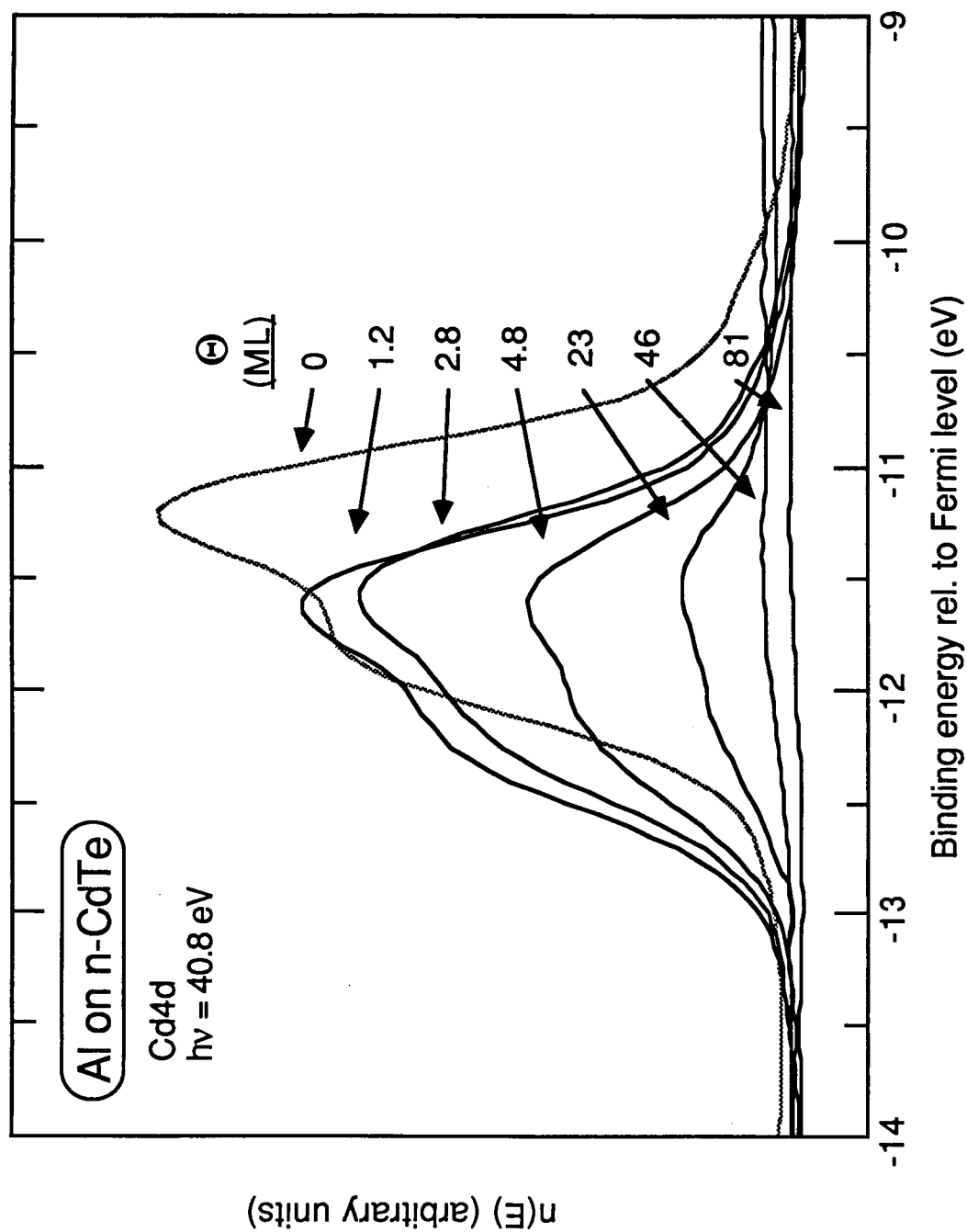


Figure 3